Differential trafficking of AMPA and NMDA receptors by SAP102 and PSD-95 underlies synapse development

G. M. Elias[a,b,1], L. A. B. Elias[a,c,1], P. F. Apostolides[b], A. R. Kriegstein[c], and R. A. Nicoll[b,d,2]

[a]Neuroscience Graduate Program, [b]Department of Cellular and Molecular Pharmacology, [c]Institute for Regeneration Medicine, and [d]Department of Physiology, University of California, San Francisco, CA 94143

Contributed by Roger A. Nicoll, November 6, 2008 (sent for review October 20, 2008)

The development of glutamatergic synapses involves changes in the number and type of receptors present at the postsynaptic density. To elucidate molecular mechanisms underlying these changes, we combine *in utero* electroporation of constructs that alter the molecular composition of developing synapses with dual whole-cell electrophysiology to examine synaptic transmission during two distinct developmental stages. We find that SAP102 mediates synaptic trafficking of AMPA and NMDA receptors during synaptogenesis. Surprisingly, after synaptogenesis, PSD-95 assumes the functions of SAP102 and is necessary for two aspects of synapse maturation: the developmental increase in AMPA receptor transmission and replacement of NR2B-NMDARs with NR2A-NMDARs. In PSD-95/PSD-93 double-KO mice, the maturational replacement of NR2B- with NR2A-NMDARs fails to occur, and PSD-95 expression fully rescues this deficit. This study demonstrates that SAP102 and PSD-95 regulate the synaptic trafficking of distinct glutamate receptor subtypes at different developmental stages, thereby playing necessary roles in excitatory synapse development.

AMPAR and NMDAR trafficking | membrane-associated guanylate kinase | synaptogenesis | postsynaptic density | synaptic transmission

A fundamental goal of developmental neurobiology is to identify the sequence of molecular events underlying excitatory synapse development, a process that can be divided into two distinct stages: synaptogenesis and synapse maturation. Synaptogenesis follows the specification of cell-to-cell contacts mediated by cell adhesion molecules (1, 2) and involves the initiation of chemical communication through the recruitment of pre- and postsynaptic proteins necessary for fast synaptic transmission (3, 4), such as AMPA receptors (AMPARs) and NMDA receptors (NMDARs). Synapse maturation is characterized by two functional events: an increase in the strength of AMPAR-mediated transmission (5, 6) and a switch in the subunit composition of synaptic NMDARs (7). NMDARs are composed of two obligatory NR1 subunits and two NR2 subunits, of which there are four members (NR2A–D) (8). NR2B-NMDARs are expressed during synaptogenesis and are replaced by NR2A-NMDARs during synapse maturation (9–11), a replacement that accounts for the developmental decrease in the NMDAR excitatory postsynaptic current (EPSC) decay time (12, 13) and the loss of sensitivity to the NR2B antagonist ifenprodil (14). The precise molecular mechanisms underlying the differential synaptic trafficking of AMPAR and NMDAR during developmental synaptogenesis and maturation remain largely unknown.

PSD-95 is a member of a family of proteins collectively known as membrane-associated guanylate kinases (MAGUKs) (15–17). The PSD-95–like subfamily of neuronal MAGUKs (PSD-MAGUKs) includes PSD-93, SAP102, and SAP97 (15–17). Comparative studies emphasize the remarkable similarities among PSD-MAGUKs in terms of protein-protein interactions (18, 19) and overlapping functions in synaptic trafficking of AMPARs at mature synapses (20–24). On the other hand, the temporal coincidence of the early postnatal developmental switch from NR2B- to NR2A-NMDARs with the switch from SAP102 to PSD-95 expression raises the possibility that the two processes are related (25). Indeed, overexpression of PSD-95 in cultured cerebellar granule cells promotes NR2A-NMDAR synaptic expression (26), and there is a greater contribution of NR2B-NMDAR–mediated transmission in juvenile PSD-95 KO mice (24). However, in another line of PSD-95 mutant mice (27), the total expression level and synaptic localization of NR2A-NMDARs in the adult hippocampus are unaffected (28). Moreover, gain-of-function (by overexpression) and loss-of-function (by shRNA-mediated knockdown) of PSD-MAGUKs in neurons cultured *in vitro* have demonstrated surprisingly little (29, 30) or no effect on the amplitude of NMDAR synaptic transmission (20, 22, 23, 31–33). Thus, the role of PSD-MAGUKs in NMDAR trafficking, if any, remains to be determined.

In the present study we elucidate distinct roles for SAP102 and PSD95 in the trafficking of both AMPA and NMDA receptors during synaptogenesis and synapse maturation.

Results

To study the molecular mechanisms underlying excitatory synapse development *in vivo*, we combined *in utero* electroporation at embryonic day 16 (E16) [supporting information (SI) Fig. S1*A*], to manipulate the expression of synaptic proteins in single hippocampal CA1 pyramidal neurons, and electrophysiology, to assay synaptic transmission using dual whole-cell recordings in acute slices at different postnatal developmental stages. Analysis of E21 (Fig. S1*B*) and postnatal day 7 (P7, Fig. S1*C*) hippocampal slices following expression of EGFP revealed a mosaic distribution of electroporated neurons ($EGFP^+$) in the CA1 region. Simultaneous dual whole-cell recordings from $EGFP^+$ and untransfected CA1 neuron pairs in acute slices revealed no difference in the amplitude of AMPAR or NMDAR EPSCs between cells (Fig. S1 *D–F*) or other measures of cellular membrane integrity, such as input resistance and series resistance (data not shown).

We studied the role of PSD-95 in synaptogenesis by *in utero* injection and electroporation of a PSD-95–EGFP lentiviral expression vector. By P7, PSD-95–EGFP overexpressing neurons were distributed throughout the hippocampal CA1 region (Fig. 1 *A* and *B*). PSD-95–EGFP molecules clustered primarily in dendrites and spine structures (Fig. 1*C*). Simultaneous dual whole-cell recordings revealed a 5-fold enhancement in the amplitude of AMPAR EPSCs in PSD-95 overexpressing neurons compared with untransfected

Author contributions: G.M.E. and R.A.N. designed research; G.M.E., L.A.B.E., and P.F.A. performed research; G.M.E., L.A.B.E., and A.R.K. contributed new reagents/analytic tools; G.M.E., L.A.B.E., and R.A.N. analyzed data; and G.M.E., L.A.B.E., and R.A.N. wrote the paper.

The authors declare no conflict of interest.

[1]G.M.E. and L.A.B.E. contributed equally to the project.

[2]To whom correspondence should be addressed at: Department of Cellular and Molecular Pharmacology, University of California, San Francisco, California 94143. E-mail: nicoll@cmp.ucsf.edu.

This article contains supporting information online at www.pnas.org/cgi/content/full/0811025106/DCSupplemental.

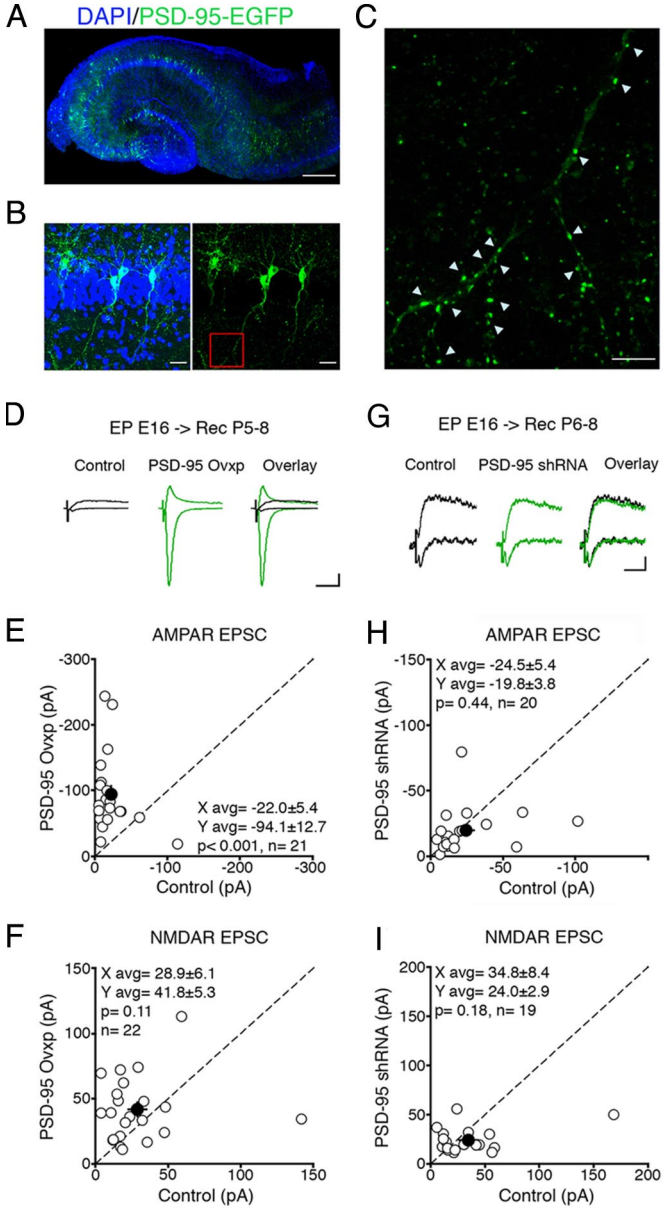

Fig. 1. PSD-95 is not necessary for synaptic trafficking of glutamate receptors during synaptogenesis *in vivo*. (*A*) Confocal image of hippocampal coronal slice at P7 after *in utero* electroporation of PSD-95–EGFP (green) at E16 (nuclear DAPI in blue). (*B*) (*Left*) CA1 region shows mosaic distribution of PSD-95 overexpressing ($EGFP^+/DAPI^+$) and untransfected neurons ($EGFP^-/DAPI^+$). (*Right*) Apical and basal dendritic arborizations of PSD-95–EGFP neurons. (*C*) Boxed area in *B* shows PSD-95–EGFP clusters (white arrowheads) in dendrites and spines. (*D*) Evoked EPSCs recorded simultaneously from an untransfected control neuron and a PSD-95 overexpressing (PSD-95 Ovxp) neighbor. (*E*, *F*, *H*, and *I*) For all EPSC scatter plots in this and subsequent figures, open and filled circles represent amplitudes for individual pairs and mean ± SEM, respectively. Distributions show a significant increase in AMPAR EPSC amplitudes (*E*) but not in NMDAR EPSC amplitudes (*F*). (*G*) Evoked EPSCs from an untransfected neuron and an adjacent neuron expressing PSD-95 shRNA. (*B*, *H*) Distributions of EPSCs show no effect of PSD-95 shRNA on AMPAR (*H*) or NMDAR (*I*) EPSC amplitudes. (Scale bars: *A*–*C* = 500, 25, and 10 μm, respectively; *D* = 50 pA, 25 ms; *G* = 10 pA, 25 ms.)

neighbors (Fig. 1 *D* and *E*). This effect was receptor selective, as the amplitude of the NMDAR-mediated EPSC component, estimated from the compound EPSCs (Fig. 1*F*) or in the presence of an AMPAR antagonist (25 μM NBQX) (Fig. S2*B*), was not significantly enhanced. Consistent with an effect specifically on postsynaptic AMPARs, the paired-pulse ratio (PPR), a measure of presynaptic release probability, did not differ between neuron groups (Fig. S3*A*). These data indicate that PSD-95 overexpression *in vivo* during synaptogenesis selectively increases the amplitude of AMPAR-mediated synaptic transmission.

To determine whether PSD-95 is necessary for synaptogenesis, we knocked down endogenous PSD-95 by *in utero* electroporation of shRNAs (23). Surprisingly, PSD-95 knockdown did not affect the amplitudes of AMPAR and NMDAR EPSCs at P6–P8 (Fig. 1 *G*–*I*) or the amplitude and frequency of AMPAR miniature excitatory postsynaptic currents (mEPSCs) (Fig. S4 *A*–*C*). Furthermore, the decay times of pharmacologically isolated NMDAR EPSCs did not differ between PSD-95 shRNA-expressing and control neurons (Fig. S3*C*), suggesting that PSD-95 does not regulate the subunit composition of NMDARs during synaptogenesis. Finally, there was no change in PPR (Fig. S3*B*). These data suggest that the overexpression effect most likely represents a gain-of-function phenotype that does not correspond to a role of endogenous PSD-95 in AMPAR trafficking during synaptogenesis.

To examine the possible role of SAP102 in glutamate receptor trafficking during synaptogenesis, we overexpressed SAP102-EGFP by *in utero* electroporation. SAP102 overexpressing neurons showed a 3-fold enhancement in AMPAR EPSC amplitude (Fig. S5 *A* and *B*) concomitant with a 2-fold increase in the amplitude of NMDAR EPSCs (Fig. 2 *A* and *B*). There was no change in PPR (Fig. 2*C*). In striking contrast to the lack of effect with PSD-95–specific shRNAs, knockdown of SAP102 reduced both AMPAR (Fig. S5 *C* and *D*) and NMDAR (Fig. 2*D*) EPSC amplitudes, without affecting PPR (Fig. 2*F*). Moreover, mEPSC analysis revealed reductions in mEPSC amplitude and frequency (Fig. S5 *E*–*G*), suggesting removal of AMPARs from all synapses.

A reduction in AMPAR and NMDAR transmission in the absence of changes in PPR could be attributed to a structural loss of spines that contain glutamate receptors. To test this, we used patch-recording pipettes to fill neighboring pairs of untransfected and SAP102 shRNA-expressing neurons simultaneously with fluorescent dyes of different emission wavelengths (Fig. 2*G*). Visualization of apical and basal dendrites as well as spines (Fig. 2*H*) enabled a pair-wise analysis of the number of spines per unit length of apical dendrite between groups. There was no difference in the number of spines (Fig. 2*I*) or total dendritic length (data not shown). These data suggest that SAP102 coregulates the synaptic trafficking of AMPARs and NMDARs during synaptogenesis rather than spine formation itself.

Is SAP102 selective or promiscuous with respect to its ability to regulate the synaptic trafficking of NR2B-NMDARs and NR2A-NMDARs? To distinguish between these possibilities, we knocked down SAP102 by *in utero* electroporation and measured the decay time of pharmacologically isolated NMDAR EPSCs at P6–P8. SAP102 knockdown reduced the peak amplitudes of NMDAR EPSCs (Fig. 3*A*1) but did not affect their decay times (Fig. 3*A*). Conversely, SAP102 overexpression during this period increased the peak amplitudes of NMDAR EPSCs (Fig. 3*B*1) but did not affect their decay times (Fig. 3*B*) or their sensitivity to ifenprodil (Fig. 3*C*). These data suggest that the NMDARs removed from, or added to, synapses by knockdown or overexpression, respectively, of SAP102 are of the same subunit composition as those present in control synapses (i.e., predominantly NR2B-NMDARs). Furthermore, overexpression of SAP102 during a developmental period when NMDAR transmission is dominated by NR2A-NMDARs (i.e., at P15–P17) increased the peak amplitude (Fig. 3*D*) but had no effect on the decay kinetics (Fig. 3*F*) of NMDAR EPSCs, suggesting that SAP102 has the ability to traffic both NR2B-NMDARs and NR2A-NMDARs. As would be expected, overexpression of SAP102 from E16 to P15–P17 significantly increased the amplitude of AMPAR EPSCs (data not shown).

To determine whether SAP102 is necessary for synapse maturation, we knocked down SAP102 *in utero* and assayed synaptic

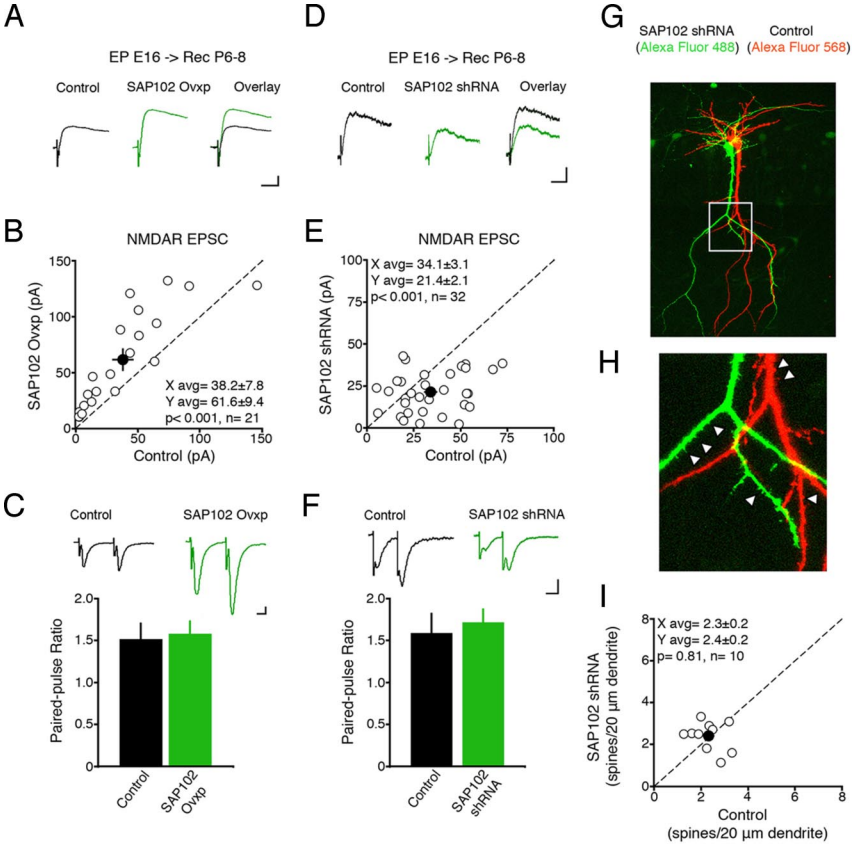

Fig. 2. SAP102 mediates NMDA receptor synaptic trafficking during synaptogenesis *in vivo*. (*A*) Representative NMDAR EPSCs from untransfected and adjacent SAP102 overexpressing (SAP102 Ovxp) neurons from E16 to P6–P8. (*B*) SAP102 overexpression significantly increases NMDAR EPSC amplitudes relative to untransfected neurons. (*D*) Representative EPSCs in untransfected and neighboring neuron expressing SAP102 shRNA. (*E*) shRNA-mediated knockdown of SAP102 significantly reduces NMDAR EPSC amplitudes. Neither SAP102 overexpression (*C*: *Top*, sample traces; *Bottom*, summary bar graph) nor SAP102 knockdown (*F*: *Top*, sample traces; *Bottom*, summary bar graph) significantly affects the PPR [(C, control: 1.5 ± 0.19, $n = 7$; SAP102 Ovxp: 1.6 ± 0.16, $n = 7$; $P = 0.82$); (F, control: 1.5 ± 0.24, $n = 8$; SAP102 shRNA: 1.7 ± 0.16, $n = 15$; $P = 0.89$)]. (Error bars = SEM.) (*G*) Confocal image of transfected (SAP102 shRNA neuron, green) and untransfected neighbor (control, red) filled with Alexa Fluors. (*H*) High magnification of boxed area in *G* shows spines in both cells (white arrowheads). (*I*) Pair-wise comparison of the number of spines per unit length of apical dendrite between SAP102 shRNA-expressing and untransfected control neurons shows no significant difference in spine density. Open and filled circles represent spine densities for single pairs and the mean ± SEM, respectively. (Scale bars: *A* = 25 pA, 25 ms; *D* = 20 pA, 25 ms.)

transmission at P15–P17. Dual whole-cell recordings revealed no difference in the amplitude of either AMPAR (Fig. S6 *A* and *B*) or peak NMDAR (Fig. 4 *A* and *B*) EPSCs in SAP102 shRNA-expressing neurons. In addition, there was no difference in the NMDAR EPSC decay kinetics between SAP102 shRNA-expressing neurons and slice-matched controls (Fig. 4*C*).

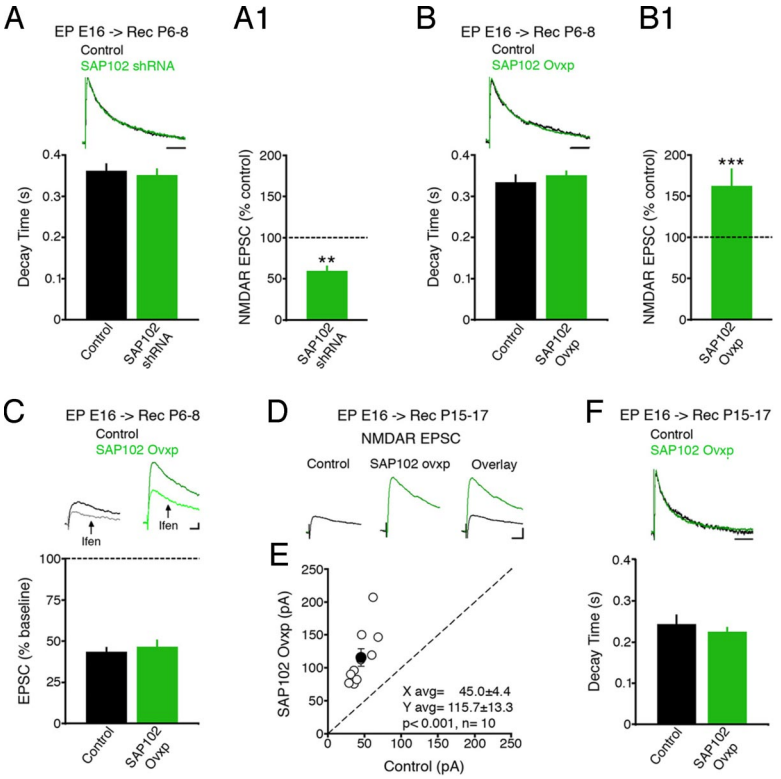

Fig. 3. SAP102 regulates synaptic insertion of NR2B-NMDARs and NR2A-NMDARs. (*A*) (*Top*) Peak-scaled NMDAR EPSCs from SAP102 shRNA-expressing and slice-matched untransfected neurons. (*Bottom*) No differences in NMDAR EPSC decay times (control: 0.36 ± 0.02 s, $n = 17$; SAP102 shRNA: 0.35 ± 0.02 s, $n = 19$; $P = 0.66$). (*A1*) SAP102 knockdown reduces NMDAR EPSC amplitudes relative to untransfected neurons (100% black dashed line) ($n = 10$; $^{**}P < 0.01$). (*B*) (*Top*) Peak-scaled NMDAR EPSCs from SAP102 overexpressing (SAP102 Ovxp) and slice-matched untransfected neurons. (*Bottom*) No significant difference in NMDAR EPSC decay time (control: 0.33 ± 0.02 s, $n = 8$; SAP102 Ovxp: 0.35 ± 0.01 s, $n = 10$; $P = 0.74$). (*B1*) SAP102 overexpression increases NMDAR EPSC amplitudes relative to untransfected neurons (100% dashed line) ($n = 21$; $^{**}P < 0.001$) (data replotted from Fig. 2*A*). (*C*) (*Top*) Traces of NMDAR EPSCs before and 20–25 min after ifenprodil application (arrow). (*Bottom*) Percent of NMDAR EPSC remaining 20–25 min after ifenprodil application relative to baseline (control: 42.95 ± 2.9%, $n = 6$; SAP102 Ovxp: 45.9 ± 4.4%, $n = 6$; $P = 0.38$). (D) NMDAR EPSCs in control and neighboring neurons overexpressing SAP102 from E16 to P15–P17. (*E*) Scatter plot shows significantly increased NMDAR EPSC peak amplitudes in SAP102 overexpressing neurons. (*F*) (*Top*) Peak-scaled NMDAR EPSCs from a SAP102 overexpressing neuron and a slice-matched untransfected neuron. (*Bottom*) Summary shows no significant difference in NMDAR EPSC decay times (control: 0.24 ± 0.02 s, $n = 11$; SAP102 Ovxp: 0.23 ± 0.01 s, $n = 11$; $P = 0.41$). (Scale bars: *A*, *B*, and *F* = 200 ms; *C* and *D* = 10 pA, 25 ms and 25 pA, 25 ms, respectively.)

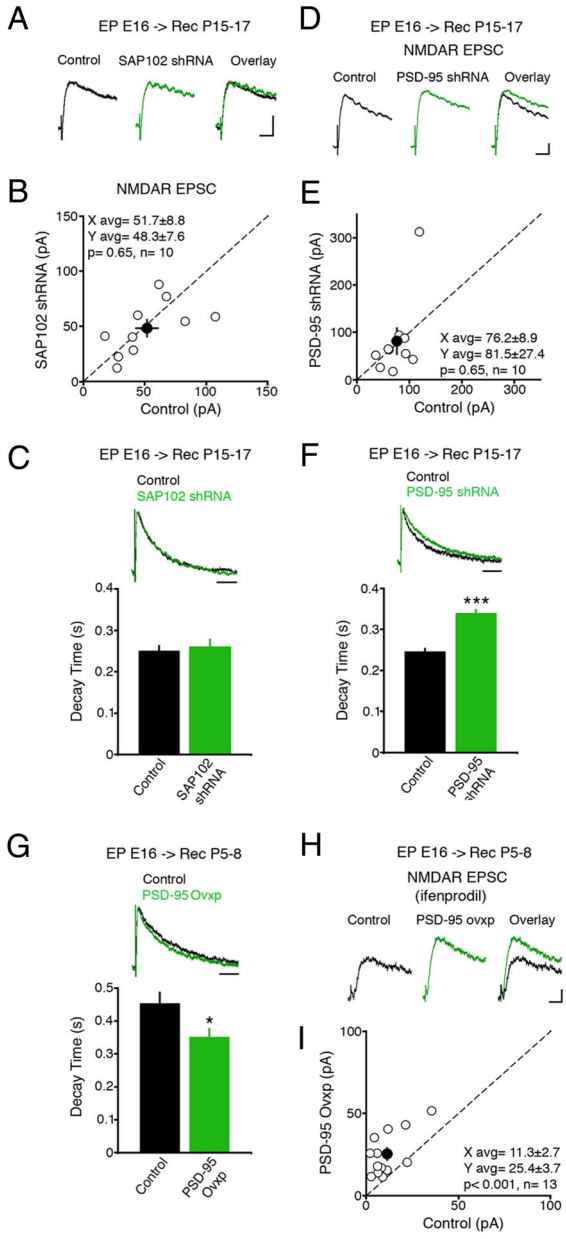

Fig. 4. PSD-95, but not SAP102, is necessary for synaptic maturation of NMDAR-mediated synaptic transmission *in vivo*. (*A*) NMDAR EPSCs in a control and a neighboring neuron expressing SAP102 shRNA. (*B*) Plot shows no significant difference in NMDAR EPSC amplitudes between conditions. (*C*) (*Top*) Peak-scaled NMDAR EPSCs recorded from a SAP102 shRNA-expressing neuron and a slice-matched untransfected control. (*Bottom*) Graph shows no significant difference in NMDAR EPSC decay times (control: 0.26 ± 0.02 s, n = 11; SAP102 shRNA: 0.25 ± 0.01 s, n = 10; P = 0.70). (*D*) NMDAR EPSCs recorded simultaneously from untransfected control and neurons expressing PSD-95 shRNA. (*E*) Plot of NMDAR EPSC peak amplitudes. (*F*) (*Top*) Peak-scaled NMDAR EPSCs recorded from a PSD-95 shRNA-expressing neuron and a slice-matched control. (*Bottom*) Graph shows a significant increase in NMDAR EPSC decay time in PSD-95 shRNA-expressing neurons (control: 0.25 ± 0.01 s, n = 16; PSD-95 shRNA: 0.34 ± 0.01 s, n = 13; ***P < 0.001). (*G*) (*Top*) Peak-scaled NMDAR EPSCs recorded from a PSD-95 overexpressing neuron (PSD-95 Ovxp) and a slice-matched control neuron. (*Bottom*) Summary shows a significant decrease in NMDAR EPSC decay time in PSD-95 overexpressing neurons (control: 0.45 ± 0.03 s, n = 17; PSD-95 Ovxp: 0.34 ± 0.03 s, n = 19; *P < 0.05). Sample traces (*H*) and scatter plot (*I*) of pharmacologically isolated NMDAR EPSCs recorded simultaneously in the presence of ifenprodil revealed a significant increase in the peak amplitude in PSD-95 overexpressing neurons relative to control. (Scale bar: *A* = 20 pA, 25 ms; *D* and *H* = 10 pA, 25 ms; *C*, *F*, and *G* = 200 ms.)

Although *in utero* expression of PSD-95 shRNAs had no effect on either AMPAR or NMDAR EPSCs when examined at P6–P8 (Fig. 1 *G–I*), there was a 50% reduction in the amplitudes of AMPAR EPSCs when examined during synaptic maturation (P15–P17) (Fig. S6 *C* and *D*). Surprisingly, although the peak amplitudes of NMDAR EPSCs did not differ between transfected and control neurons (Fig. 4 *D* and *E*), PSD-95 knockdown significantly increased the decay time of NMDAR EPSCs (Fig. 4*F*), suggesting that PSD-95 is necessary for the increase in the fraction of synaptic NR2A-NMDARs that occurs during synapse maturation. Indeed, PSD-95 overexpression from E16 to P5–P8 significantly decreased the decay time of NMDAR EPSCs (Fig. 4*G*), suggesting that PSD-95 overexpression is sufficient to promote a premature switch in synaptic NMDARs from NR2B- to NR2A-containing NMDARs. In addition, although PSD-95 overexpression did not change the overall peak amplitude of NMDAR responses (Fig. 1*F* and Fig. S2*B*), it increased the peak amplitude of the NR2A-NMDAR EPSCs recorded in the presence of ifenprodil (Fig. 4 *H–I*). As expected, isolated NR2A-NMDAR responses had the same decay time in both the PSD-95–EGFP-expressing and control neurons, suggesting that the decrease in the decay kinetics (Fig. 4*G*) is, in fact, attributable to a reduction in the proportion of NR2B-NMDARs (Fig. S6*E*). These findings indicate that in addition to promoting insertion of NR2A-NMDARs, PSD-95 overexpression reduces the number of NR2B-NMDARs while keeping the total number of NMDARs at the synapse constant. Thus, PSD-95 coregulates the synaptic trafficking of AMPARs and the exchange of NR2B-NMDARs for NR2A-NMDARs.

Whereas germline deletion of PSD-95 or PSD-93 does not affect AMPAR- or NMDAR-mediated synaptic transmission between P30 and P40, PSD-95$^{-/-}$/PSD-93$^{-/-}$ mice show a profound deficit in AMPAR transmission at this age (23). In contrast, we found no differences in NMDAR-mediated field EPSPs between genotypes (Fig. 5*A*). Whereas NMDAR EPSC decay times were normal in PSD-95$^{-/-}$ or PSD-93$^{-/-}$ mice (Fig. 5*B*), they were significantly increased in PSD-95$^{-/-}$/PSD-93$^{-/-}$ mice (Fig. 5*B*). In addition, the percent block of NMDAR EPSCs by ifenprodil in PSD-95$^{-/-}$/PSD-93$^{-/-}$ mice was significantly greater than in control (Fig. 5*C*). These data suggest that germ line deletion of PSD-95 and PSD-93 prevents the maturational switch from NR2B- to NR2A-NMDARs.

Can PSD-95 expression in PSD-95$^{-/-}$/PSD-93$^{-/-}$ neurons rescue synapse maturation? PSD-95 overexpression (31) in WT and PSD-95$^{-/-}$/PSD-93$^{-/-}$ slice cultures increased AMPAR EPSCs by 3-fold (Fig. S7 *A* and *B*) and 6-fold (Fig. 5 *D* and *E*), respectively. PSD-95 overexpression did not affect the peak amplitudes of NMDAR EPSCs in either WT (Fig. S7 *A* and *B*) or PSD-95$^{-/-}$/PSD-93$^{-/-}$ (Fig. 5 *D* and *E*) mice. The NMDAR EPSC decay times in WT slice cultures were similar to those measured at mature synapses in acute slices from adult mice, and PSD-95 overexpression did not affect the decay times (Fig. 5*F*). In contrast, NMDAR EPSC decay times in PSD-95$^{-/-}$/PSD-93$^{-/-}$ slice cultures were significantly slower relative to WT, and PSD-95 expression was sufficient to restore the decay time to WT levels (Fig. 5*G*). This suggests that in the absence of PSD-95 and PSD-93, excitatory synapses remain in an immature state that can be rescued by restoring PSD-95 expression.

Discussion

In the present study, we find that SAP102 and PSD-95 have distinct roles during synaptogenesis and synapse maturation. This segregation of function occurs by two mechanisms. First, SAP102, which is already expressed by P2 (34), is primarily responsible for AMPAR and NMDAR trafficking during synaptogenesis, whereas PSD-95 is not necessary for synaptic trafficking during this developmental window. Second, although SAP102 is devoid of NR2 selectivity and

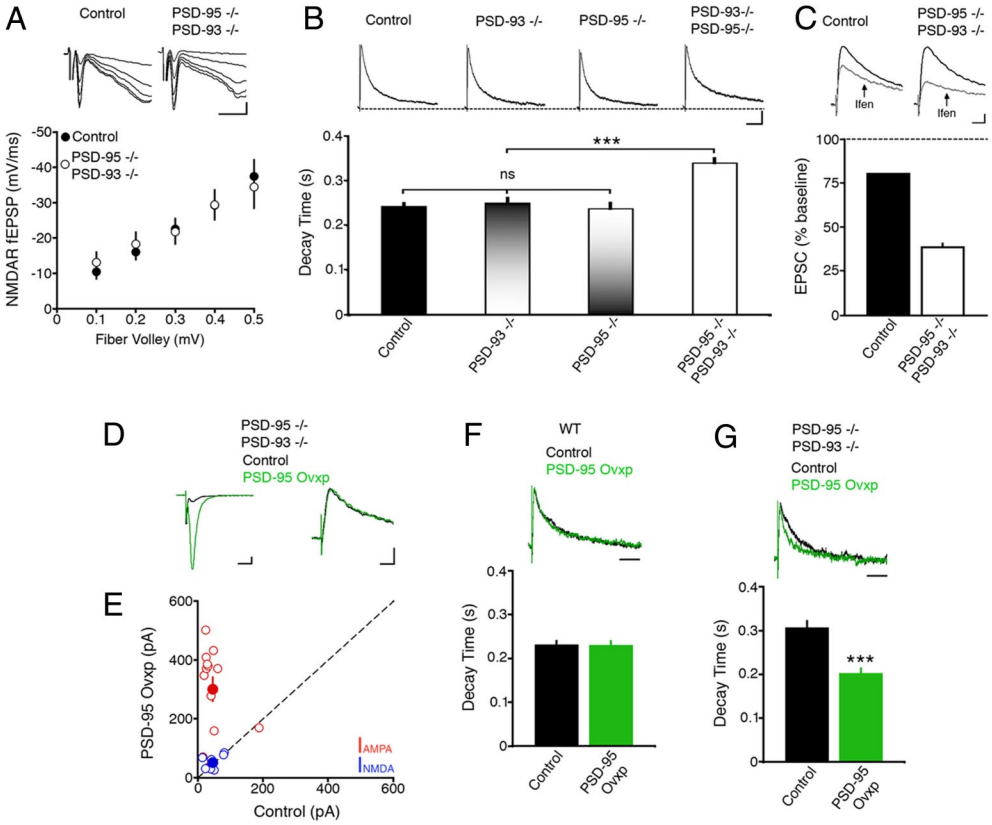

Fig. 5. PSD-95 expression rescues deficit in synapse maturation in PSD-95$^{-/-}$/PSD-93$^{-/-}$ mice. (*A*) NMDAR-mediated field EPSPs (*Top*) and input-out curve (*Bottom*) show that for each input (fiber volley [FV]), the output (field EPSP slope) is unchanged. Each point represents mean ± SEM for each FV (control: $n = 22$, 24, 20, 19, and 17 slices for FVs 0.1, 0.2, 03, 0.4, and 0.5 mV, respectively; PSD-95$^{-/-}$/PSD-93$^{-/-}$: $n = 24$, 23, 19, 19, and 10 slices for FVs 0.1, 0.2, 03, 0.4, and 0.5 mV, respectively; $P > 0.05$ for all FVs). (*B*) (*Top*) NMDAR EPSCs recorded from P30–P40 mice. (*Bottom*) Graph shows a significant increase in NMDAR EPSC decay time in PSD-95$^{-/-}$/PSD-93$^{-/-}$ (control: 0.24 ± 0.01 s, $n = 10$; PSD-93$^{-/-}$: 0.25 ± 0.01 s, $n = 10$; PSD-95$^{-/-}$: 0.24 ± 0.74 s, $n = 13$; PSD-95$^{-/-}$/PSD-93$^{-/-}$: 0.34 ± 0.01 s, $n = 10$; ns $P > 0.05$; ***$P < 0.001$). (*C*) (*Top*) NMDAR EPSCs recorded before (black traces) and 20–25 min after (arrow, gray traces) ifenprodil application. (*Bottom*) Percent of NMDAR EPSC remaining after ifenprodil application relative to baseline (control: 80%; PSD-95$^{-/-}$/PSD-93$^{-/-}$: 38.5 ± 2.1%, $n = 10$). (*D*) AMPAR (*Left*) and NMDAR (*Right*) EPSCs recorded simultaneously from PSD-95 overexpressing (PSD-95 Ovxp) and uninfected control neurons in PSD-95$^{-/-}$/PSD-93$^{-/-}$ slice cultures. (*E*) Scatter plot demonstrates that PSD-95 overexpression significantly increases AMPAR EPSC (red circles) amplitudes (control: −45.85 ± 12.39 pA; PSD-95 Ovxp: −301.15 ± 40.44 pA; $n = 13$ pairs; ***$P < 0.001$), without affecting NMDAR EPSC (blue circles) peak amplitudes (control: 45.92 ± 8.47 pA; PSD-95 Ovxp: 52.21 ± 8.46 pA; $n = 8$ pairs; $P = 0.46$). (*F*) (*Top*) Peak-scaled NMDAR EPSCs recorded from PSD-95 overexpressing and slice-matched untransfected neurons. (*Bottom*) No significant difference in NMDAR EPSC decay times (control: 0.23 ± 0.01 s, $n = 15$; PSD-95 Ovxp: 0.23 ± 0.01 s; $n = 12$; $P = 0.96$). (*G*) (*Top*) Peak-scaled NMDAR EPSCs recorded from PSD-95$^{-/-}$/PSD-93$^{-/-}$ neurons overexpressing PSD-95 and slice-matched untransfected control. (*Bottom*) Graph shows a significant decrease in NMDAR EPSC decay time in PSD-95$^{-/-}$/PSD-93$^{-/-}$ neurons expressing PSD-95 (control: 0.31 ± 0.02 s, $n = 20$; PSD-95 Ovxp: 0.20 ± 0.01 s; $n = 10$; ***$P < 0.001$). (Scale bars: *A* = 0.1 mV, 5 ms; *B* = 20 pA, 200 ms, *C* = 10 pA, 25 ms; *D* = 25 pA, 25 ms; *F* and *G* = 200 ms.)

can mediate synaptic trafficking of NR2B- and NR2A-NMDARs during synaptogenesis, the maturational switch of NR2B-NMDARs to NR2A-NMDARs is regulated by PSD-95. Furthermore, PSD-95 regulates the increase in the number of synaptic AMPARs during synapse maturation. Interestingly, the mechanisms of glutamate receptor trafficking mediated by SAP102 during synaptogenesis appear to be fundamentally different from those at play in mature synapses: in contrast to the knockdown of PSD-95 in mature synapses, in which AMPA receptors are removed in an all-or-none fashion from a subset of synapses (23, 24), knockdown of SAP102 during synaptogenesis causes a uniform removal of AMPARs from all synapses.

The lack of effect of PSD-95 knockdown on synapse function during synaptogenesis is presumably attributable to a lack of PSD-95 expression at this developmental stage, because the embryonic overexpression of PSD-95 dramatically enhances AMPAR EPSCs. Indeed, glutamatergic synaptic transmission in 1-week-old PSD-95$^{-/-}$ (24) and PSD-95$^{-/-}$/PSD-93$^{-/-}$ mice (23) appears normal, and EM immunogold labeling studies *in vivo* show little PSD-95 during the first 2 postnatal weeks (34). These *in vivo* findings are seemingly at odds with a number of *in vitro* studies, largely from dissociated neuronal cultures, claiming that PSD-95 is one of the earliest proteins to appear at developing synapses (3, 4). This difference may reflect different experimental conditions or the possibility that the antibodies used cross-reacted with SAP102 and/or other synaptic proteins.

Unexpectedly, although SAP102 is necessary for the trafficking of AMPARs and NMDARs during synaptogenesis, synapse maturation is not impaired by the early knockdown of SAP102. This implies that the programs involved in synaptogenesis and maturation are independent or that in the absence of SAP102, the increasing levels of other PSD-MAGUKs, such as PSD-95 or PSD-93, during maturation can compensate for this perturbation. It is also possible that PSD-93 might account for the remaining transmission under SAP102 knockdown conditions. Although overexpression of SAP102 at mature synapses has no effect on the amplitude of the NMDAR EPSC (20), overexpression during synaptogenesis does and this increase persists throughout synapse maturation. This suggests that the number of NMDARs that can be inserted during synaptogenesis by SAP102 is not limited but that once the synapse has matured, there is a ceiling and additional NMDARs cannot be inserted into the synapse. This is similar to the activity-dependent switching of NR2B-NMDARs with NR2A-NMDARs (7). It will be of interest to determine how activity engages this PSD-95/NR2A switching mechanism.

Perhaps the most striking finding presented here is the differential action of SAP102 and PSD-95 on NMDAR synaptic trafficking. We found that SAP102 can traffic both NR2A- and NR2B-NMDARs, whereas PSD-95 is only capable of trafficking NR2A-NMDARs. In light of this, the predominance of NR2B-NMDARs at synapses during synaptogenesis is likely attributable to their selective expression during this period. However, the reason why SAP102, but not PSD-95, can traffic NR2B-NMDARs remains to be explained. This functional selectivity is particularly intriguing in light of biochemical evidence suggesting that PSD-95 and SAP102 are both able to interact with di-heteromeric NR1-NR2A

and NR1-NR2B NMDARs (19). This binding promiscuity suggests that the segregation of function between SAP102 and PSD-95 may be mediated by an unknown intermediary protein.

Postsynaptic expression of PSD-MAGUKs in immature dissociated neuronal cultures has been shown to enhance presynaptic function (35, 36). We found that changing the levels of PSD-95 (or SAP102) during synaptogenesis or synapse maturation did not affect the PPR, suggesting that neither PSD-95 nor SAP102 retrogradely regulates presynaptic function *in vivo*.

Previous studies have emphasized similarities among PSD-MAGUK family members with respect to synaptic trafficking of AMPARs. The present study establishes distinct, isotype-specific roles for SAP102 and PSD-95 during synapse development. This raises the possibility that different PSD-MAGUKs may play distinct functional roles in other processes involving synaptic trafficking of glutamate receptor, for example, during activity dependent synaptic plasticity.

Methods

***In Utero* Intraventricular Injection and Electroporation of Plasmid Constructs.** Expression vectors were introduced into the developing cortex *in vivo* by intraventricular injection and electroporation as previously described (37, 38). The following shRNA targeting sequences for PSD-95 and SAP102 were used: TCACGATCATCGCTCAGTATA for PSD-95 and CCAAGTCCATCGAAGCACTTA for SAP102 (see *SI Methods*).

Live Cell Dye Filling and Confocal Imaging. Adjacent transfected and untransfected neuron pairs were visually identified in 300-μm-thick acute slices of electroporated hippocampi. Recording pipettes, filled with internal recording solution supplemented with 500 μM Alexa Fluor 488 or Alexa Fluor 568, were used to fill cells (see *SI Methods*).

Electrophysiological Recording Conditions.

Dual Whole-Cell Recordings in Acute Slices After Electroporation. For all EPSC scatter plots, open and filled circles represent amplitudes for individual pairs and mean $\pm$ SEM, respectively. Transverse hippocampal slices (300 μm thick) were prepared from electroporated pups ranging from P5–P17 (see text). Recordings were done at room temperature (25–28 °C) in artificial cerebrospinal fluid supplemented with 0.1–0.15 mM picrotoxin and, depending on the experiment, 3 μM ifenprodil (to block NR2B-NMDARs), 25 μM NBQX (to isolate NMDAR responses), TTX (to measure mEPSCs), or a combination of these drugs (see text for details).

Electrophysiological Recordings in Mouse Acute Slices. Recordings were performed from P30–P40. To minimize variability, slices from each knockout genotype and control were interleaved in a given day.

Electrophysiological Recordings in Slice Culture. Mouse organotypic slice cultures were prepared from animals ranging from P6–P8 (20, 31). Statistical significance was determined using two-tailed paired *t* tests (for EPSC amplitude comparisons in simultaneous paired recordings) or unpaired *t* tests (for NMDAR field EPSP and decay time comparisons). For mEPSC, statistical significance between distributions was determined using the Kolmogorov-Smirnov test (see *SI Methods* for additional information).

ACKNOWLEDGMENTS. We thank William Walantus, Grant Li, and Sam Pleasure for advice and assistance with *in utero* electroporation techniques; Carryn Barker for immunohistochemical assistance; and members of the Nicoll laboratory for insightful comments. We also thank Wei Lu and Eric Schnell for specific suggestions on the manuscript. This work was funded by grants from the National Institutes of Health (to R.A.N. and A.R.K.) and the California Institute of Regenerative Medicine (to L.A.B.E.). G.M.E. is supported by the University of California, San Francisco Chancellor Graduate Award and the University of California President Dissertation-Year Award.

1. Washbourne P, *et al.* (2004) Cell adhesion molecules in synapse formation. *J Neurosci* 24:9244–9249.
2. Craig AM, Graf ER, Linhoff MW (2006) How to build a central synapse: Clues from cell culture. *Trends Neurosci* 29:8–20.
3. McAllister AK (2007) Dynamic aspects of CNS synapse formation. *Annu Rev Neurosci* 30:425–450.
4. Waites CL, Craig AM, Garner CC (2005) Mechanisms of vertebrate synaptogenesis. *Annu Rev Neurosci* 28:251–274.
5. Wu G, Malinow R, Cline HT (1996) Maturation of a central glutamatergic synapse. *Science* 274:972–976.
6. Petralia RS, *et al* (1999) Selective acquisition of AMPA receptors over postnatal development suggests a molecular basis for silent synapses. *Nat Neurosci* 2:31–36.
7. Bellone C, Nicoll RA (2007) Rapid bidirectional switching of synaptic NMDA receptors. *Neuron* 55:779–785.
8. Cull-Candy SG, Leszkiewicz DN (2004) Role of distinct NMDA receptor subtypes at central synapses. *Sci STKE* re16.
9. Monyer H, Burnashev N, Laurie DJ, Sakmann B, Seeburg PH (1994) Developmental and regional expression in the rat brain and functional properties of four NMDA receptors. *Neuron* 12:529–540.
10. Sheng M, Cummings J, Roldan LA, Jan YN, Jan LY (1994) Changing subunit composition of heteromeric NMDA receptors during development of rat cortex. *Nature* 368:144–147.
11. Flint AC, Maisch US, Weishaupt JH, Kriegstein AR, Monyer H (1997) NR2A subunit expression shortens NMDA receptor synaptic currents in developing neocortex. *J Neurosci* 17:2469–2476.
12. Carmignoto G, Vicini S (1992) Activity-dependent decrease in NMDA receptor responses during development of the visual cortex. *Science* 258:1007–1011.
13. Hestrin S (1992) Developmental regulation of NMDA receptor-mediated synaptic currents at a central synapse. *Nature* 357:686–689.
14. Kirson ED, Yaari Y (1996) Synaptic NMDA receptors in developing mouse hippocampal neurones: Functional properties and sensitivity to ifenprodil. *J Physiol* (London) 497:437–455.
15. Elias GM, Nicoll RA (2007) Synaptic trafficking of glutamate receptors by MAGUK scaffolding proteins. *Trends Cell Biol* 17:343–352.
16. Funke L, Dakoji S, Bredt DS (2005) Membrane-associated guanylate kinases regulate adhesion and plasticity at cell junctions. *Annu Rev Biochem* 74:219–245.
17. Sheng M, Sala C (2001) PDZ domains and the organization of supramolecular complexes. *Annu Rev Neurosci* 24:1–29.
18. Irie M, *et al.* (1997) Binding of neuroligins to PSD-95. *Science* 277:1511–1515.
19. Al-Hallaq RA, Conrads TP, Veenstra TD, Wenthold RJ (2007) NMDA di-heteromeric receptor populations and associated proteins in rat hippocampus. *J Neurosci* 27:8334–8343.
20. Schnell E, *et al.* (2002) Direct interactions between PSD-95 and stargazin control synaptic AMPA receptor number. *Proc Natl Acad Sci USA* 99:13902–13907.
21. Nakagawa T, *et al.* (2004) Quaternary structure, protein dynamics, and synaptic function of SAP97 controlled by L27 domain interactions. *Neuron* 44:453–467.
22. Schluter OM, Xu W, Malenka RC (2006) Alternative N-terminal domains of PSD-95 and SAP97 govern activity-dependent regulation of synaptic AMPA receptor function. *Neuron* 51:99–111.
23. Elias GM, *et al.* (2006) Synapse-specific and developmentally regulated targeting of AMPA receptors by a family of MAGUK scaffolding proteins. *Neuron* 52:307–320.
24. Beique JC, *et al.* (2006) Synapse-specific regulation of AMPA receptor function by PSD-95. *Proc Natl Acad Sci USA* 103:19535–19540.
25. van Zundert B, Yoshii A, Constantine-Paton M (2004) Receptor compartmentalization and trafficking at glutamate synapses: A developmental proposal. *Trends Neurosci* 2:428–437.
26. Losi G, *et al.* (2003) PSD-95 regulates NMDA receptors in developing cerebellar granule neurons of the rat. *J Physiol* (London) 548:21–29.
27. Migaud M, *et al.* (1998) Enhanced long-term potentiation and impaired learning in mice with mutant postsynaptic density-95 protein. *Nature* 396:433–439.
28. Park CS, Elgersma Y, Grant SG, Morrison JH (2008) alpha-Isoform of calcium-calmodulin-dependent protein kinase II and postsynaptic density protein 95 differentially regulate synaptic expression of NR2A- and NR2B-containing N-methyl-D-aspartate receptors in hippocampus. *Neuroscience* 151:43–55.
29. Futai K, *et al.* (2007) Retrograde modulation of presynaptic release probability through signaling mediated by PSD-95-neuroligin. *Nat Neurosci* 10:186–195.
30. Ehrlich I, Klein M, Rumpel S, Malinow R (2007) PSD-95 is required for activity-driven synapse stabilization. *Proc Natl Acad Sci USA* 104:4176–4181.
31. Stein V, House DR, Bredt DS, Nicoll RA (2003) Postsynaptic density-95 mimics and occludes hippocampal long-term potentiation and enhances long-term depression. *J Neurosci* 23:5503–5506.
32. Beique JC, Andrade R (2003) PSD-95 regulates synaptic transmission and plasticity in rat cerebral cortex. *J Physiol* (London) 546:859–867.
33. Ehrlich I, Malinow R (2004) Postsynaptic density 95 controls AMPA receptor incorporation during long-term potentiation and experience-driven synaptic plasticity. *J Neurosci* 24:916–927.
34. Sans N, *et al.* (2000) A developmental change in NMDA receptor-associated proteins at hippocampal synapses. *J Neurosci* 20:1260–1271.
35. El-Husseini AE, Schnell E, Chetkovich DM, Nicoll RA, Bredt DS (2000) PSD-95 involvement in maturation of excitatory synapses. *Science* 290:1364–1368.
36. Regalado MP, Terry-Lorenzo RT, Waites CL, Garner CC, Malenka RC (2006) Transsynaptic signaling by postsynaptic synapse-associated protein 97. *J Neurosci* 26:2343–2357.
37. Saito T, Nakatsuji N (2001) Efficient gene transfer into the embryonic mouse brain using in vivo electroporation. *Dev Biol* 240:237–246.
38. Noctor SC, Flint AC, Weissman TA, Dammerman RS, Kriegstein AR (2001) Neurons derived from radial glial cells establish radial units in neocortex. *Nature* 409:714–720.